Stochastic Representation of Non-Markovian Fermionic Quantum Dissipation

Lu Han,[1] Vladimir Chernyak,[1,2] Yun-An Yan,[3] Xiao Zheng,[1,*] and YiJing Yan[4]

[1]*Hefei National Laboratory for Physical Sciences at the Microscale & Synergetic Innovation Center of Quantum Information and Quantum Physics & CAS Center for Excellence in Nanoscience, University of Science and Technology of China, Hefei, Anhui 230026, China*

[2]*Department of Chemistry, Wayne State University, 5101 Cass Avenue, Detroit, Michigan 48202, USA*

[3]*School of Physics and Optoelectronic Engineering, Ludong University, Shandong 264025, China*

[4]*Hefei National Laboratory for Physical Sciences at the Microscale & iChEM, University of Science and Technology of China, Hefei, Anhui 230026, China*

(Received 26 June 2018; published 31 July 2019)

Quantum Brownian motion plays a fundamental role in many areas of modern physics. In the path-integral formulation, environmental fluctuations can be characterized by auxiliary stochastic fields. Intriguingly, for fermionic environments the stochastic fields must be Grassmann valued so as to memorize the order of the random forces exerted on the system. Such nonclassical fields cannot be represented by conventional means. We propose a strategy to map the Grassmann-number fields to conventional c-number noises and a set of quantized pseudolevels. The resulting stochastic equation of motion (SEOM) enables direct stochastic simulation of the fermionic dissipative dynamics. The SEOM gives exact physical observables of noninteracting systems, and yields accurate approximate results for interacting systems. The practicality and accuracy of the proposed strategy and the SEOM are exemplified by numerical studies conducted on a single-impurity Anderson model.

DOI: 10.1103/PhysRevLett.123.050601

Introduction.—Over a century ago, Einstein explained the nature of Brownian motion by establishing a quantitative relationship between the dissipative forces driving a classical particle and the environmental thermal fluctuations [1]. Nowadays, quantum Brownian motion [2–6], i.e., the dissipative dynamics of a quantum system driven by the quantum fluctuations in the surrounding environments [7], plays a fundamental role in many subdisciplines of modern physics.

The main challenge in describing quantum Brownian motion is to address the combined effects of system-environment dissipation [8], many-body interaction [9], and non-Markovian memory [10,11]. This requires a statistical treatment of environment which usually has an infinite number of degrees of freedom. The environmental fluctuations have been characterized by a number of principal pseudomodes [12,13] or "dissipatons" [14], leading to a coupled set of Fokker-Planck-type equations, such as the hierarchical equations of motion (HEOM) [15–18]. However, in certain circumstances, such as when the environmental temperature is low, the set of deterministic equations can be too large to be practical.

Alternatively, environmental fluctuations can be captured by stochastic fields [19]. The Brownian dynamics of a quantum pollen grain, and more generally, the dissipative dynamics of an open quantum system, can be formally described by a Langevin-type equation (we set $\hbar = 1$ in below) [20,21]:

$$|\dot{\Psi}_{\rm s}\rangle = -iH_S|\Psi_{\rm s}\rangle + v_t\hat{L}|\Psi_{\rm s}\rangle. \tag{1}$$

Here, $|\Psi_{\rm S}\rangle$ and H_S are the wave function and Hamiltonian of the system, respectively. The stochastic field v_t together with the integro-differential operator $\hat{L}$ constitute the random force exerted by the environment.

Figure 1 illustrates the time evolution of a system-bath composite driven by stochastic fluctuations in the bath. The dissipation events are the transfer of particles from the bath to the system. If the particles are bosons, interchanging the order of two bath fluctuations will not change the statistical average of the final state, provided that $\{v_t\}$ are *classical* fields, i.e., $v_t v_\tau = v_\tau v_t$. Therefore, for a boson bath, the stochastic fields in Eq. (1) can be represented by c-number noises. Such formal simplicity has greatly facilitated the development and application of the stochastic theories for bosonic environments. For instance, the quantum state diffusion (QSD) theory [20,22–29] and the stochastic equation of motion (SEOM) theory [21,30–35] have been applied to investigate the quantum dissipative dynamics in realistic systems, such as the transfer of excitons in molecular aggregates under the influence of a phonon bath [36].

The situation is different for fermionic environments. As exemplified in Fig. 1, if $\{v_t\}$ were classical fields, interchanging the order of two bath fluctuations would result in a sign change in the final wave function. This is obviously unphysical, because the sign change would lead to a nonunique statistical average of the final state.

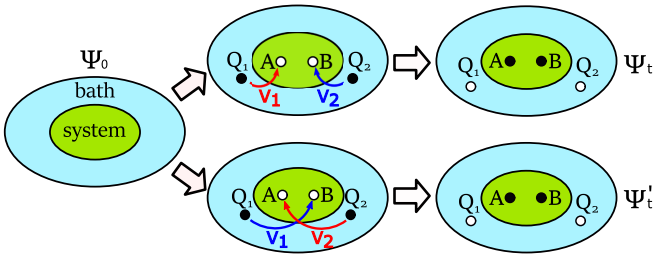

FIG. 1. Illustration of time evolution of a system-bath composite driven by stochastic fluctuations in the bath. For simplicity, the composite Hamiltonian is set to zero. The upper branch involves two dissipation events: a particle transfers from Q_1 (in the bath) to A (in the system) at time t_1 driven by v_1, and a second particle transfers from Q_2 to B at time t_2 driven by v_2, where v_1 and v_2 are two arbitrary dimensionless noises. The final state is $|\Psi_t\rangle = |\Phi_t\rangle - v_2 v_1 \hat{d}_B^\dagger \hat{d}_{Q_2} \hat{d}_A^\dagger \hat{d}_{Q_1} |\Psi_0\rangle$, where $|\Psi_0\rangle$ is the initial state and $|\Phi_t\rangle$ contains the rest of $|\Psi_t\rangle$. In the lower branch, the order of the two bath fluctuations is interchanged, and the final state is $|\Psi'_t\rangle = |\Phi'_t\rangle - v_1 v_2 \hat{d}_B^\dagger \hat{d}_{Q_1} \hat{d}_A^\dagger \hat{d}_{Q_2} |\Psi_0\rangle$. Here, $\hat{d}_{Q_1}$ and $\hat{d}_{Q_2}$ commute (anticommute) for a boson (fermion) bath. To ensure $|\Psi_t\rangle$ and $|\Psi'_t\rangle$ have the same statistical average over $\{v_1, v_2, Q_1, Q_2\}$, we must have $v_2 v_1 = v_1 v_2$ for the boson bath, and $v_2 v_1 = -v_1 v_2$ for the fermion bath, respectively. More details are given in the Supplemental Material [37]. $|\Psi_s\rangle$ in Eq. (1) is obtained by further tracing out the bath degrees of freedom in $|\Psi_t\rangle$.

Therefore, to preserve the uniqueness of all the physical observables, $\{v_t\}$ must satisfy $v_t v_\tau = -v_\tau v_t$. This means that the stochastic fields should contain the information on the order of all the bath fluctuations prior to the final time. Mathematically, such *nonclassical* fields are represented by Grassmann-number (g number) noises.

Unlike c numbers, the g numbers cannot be realized by scalars. Normally, it would require N matrices of size $2^N \times 2^N$ to represent N anticommuting g numbers, which is apparently impractical when N is large. Such difficulty has severely hindered the practical application of stochastic theories to fermionic environments. From the early formulation of fermion Brownian motion [38–41] to the recent extensions of QSD [42–46] and SEOM [47] theories to fermionic open systems, all the previous efforts were limited to formal derivations [42,47], whereas to the best of our knowledge, no stochastic simulation has been conducted on the fermionic dissipative dynamics.

To enable direct stochastic simulation of fermion Brownian motion, we need to overcome three problems: First, the bath's infinite degrees of freedom are to be decoupled from the system dynamics. Second, the influence of non-Markovian bath memory on the system state needs to be accounted for properly. Third, the g-number fields representing the stochastic bath fluctuations must be realized numerically. While the first and second problems are common to boson baths, the third problem is unique and formidable to fermion baths.

A new mapping strategy.—To interrupt the status quo, and to conquer the above three problems, we propose in this Letter a new mapping strategy consisting of three consecutive mappings, through which a numerically feasible and accurate SEOM method for fermionic open systems is finally established.

As depicted in Fig. 2, through the mapping (i), the system-bath coupling is replaced by stochastic g-number fields applied on the system and the bath. This formally decouples the system dynamics from the bath counterpart. However, after the mapping (i), the fermion bath still has an indirect influence on the statistical average of the system state through its non-Markovian memory.

The mapping (ii) is subsequently adopted to capture the non-Markovian bath memory. This gives rise to the memory-convoluted g-number fields applied on the system. After the mapping (ii), the statistical average of the system state no longer depends explicitly on the bath's degrees of freedom.

The bosonic analogues of the mappings (i) and (ii) have been developed [21,31], but with the stochastic fields being c numbers. They have allowed for stochastic simulation of bosonic dissipative dynamics. In contrast, for fermionic environments the mappings (i) and (ii) alone are inadequate because of the aforementioned formidable difficulty in numerical realization of the g numbers. To overcome this problem, we propose a new mapping, the mapping (iii), through which the g-number fields are represented by c numbers and a set of pseudolevels; see Fig. 2. This eliminates the difficulty haunting the stochastic simulation

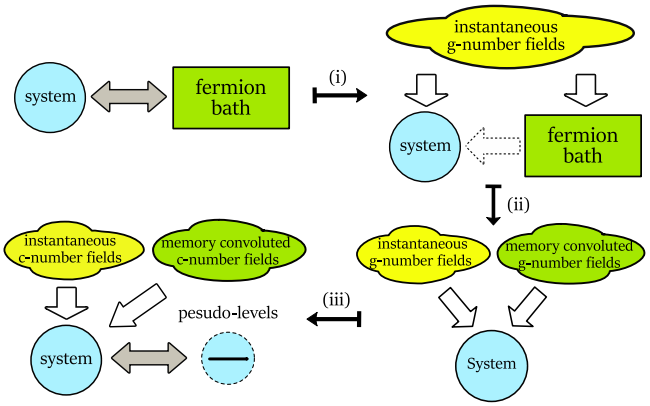

FIG. 2. Schematic illustration of our strategy to enable direction simulation of fermionic dissipative systems. Through the mapping (i), the system-bath coupling is replaced by stochastic g-number fields applied on both the system and the fermion bath. The dotted arrow indicates the influence of non-Markovian bath memory on the statistical average of the system state. Through the mapping (ii), the non-Markovian bath memory is captured by the memory-convoluted g-number fields applied on the system. Through the mapping (iii), all the g-number fields are represented by stochastic c-number fields and a set of pseudolevels. The mappings (i)–(iii) finally result in a numerically feasible SEOM.

of fermionic open systems, and eventually results in a numerically feasible SEOM. In the following, we elaborate on the details of the mappings (i)–(iii).

Mapping (i): Decoupling system from bath.—Without loss of generality, we apply our strategy to a single-level system (described by $H_S = \epsilon\hat{c}^\dagger\hat{c}$) initially isolated from a fermion bath (described by H_B). The system-bath coupling is then turned on as $H_{SB} = \hat{c}^\dagger\hat{F} + \hat{F}^\dagger\hat{c}$ with $\hat{F} = \sum_k t_k\hat{d}_k$. Here, $\{t_k\}$ are coupling strengths, and $\hat{c}$ ($\hat{c}^\dagger$) and $\hat{d}_k$ ($\hat{d}_k^\dagger$) are the annihilation (creation) operators for the system and bath levels, respectively.

In the path-integral formulation, we factorize the propagators $e^{\pm iH_{SB}\mathrm{d}t}$ by employing a stochastic decoupling approach [31]. This results in a Langevin-type equation for the decoupled system or bath density matrix ρ_S/ρ_B [37]:

$$\dot{\rho}_S = -i[H_S,\rho_S] + e^{-i\pi/4}(\hat{c}^\dagger\eta_{1t} + \bar{\eta}_{2t}\hat{c})\rho_S + e^{i\pi/4}\rho_S(\hat{c}^\dagger\eta_{3t} + \bar{\eta}_{4t}\hat{c}), \tag{2}$$

$$\dot{\rho}_B = -i[H_B,\rho_B] + e^{-i\pi/4}(\bar{\eta}_{1t}\hat{F} + \hat{F}^\dagger\eta_{2t})\rho_B + e^{i\pi/4}\rho_B(\bar{\eta}_{3t}\hat{F} + \hat{F}^\dagger\eta_{4t}). \tag{3}$$

Hereafter, we use $\{\eta_{jt}\}$ to denote the auxiliary g-number fields (AGFs), and $\bar{\eta}_{jt}$ is the conjugate of η_{jt}. The AGFs should satisfy $\eta_{jt}\eta_{j'\tau} = -\eta_{j'\tau}\eta_{jt}$, and their stochastic averages are $\langle\eta_{jt}\rangle = \langle\bar{\eta}_{jt}\rangle = 0$ and $\langle\eta_{jt}\bar{\eta}_{j'\tau}\rangle = \delta_{jj'}\delta(t-\tau)$.

Being the outcomes of the mapping (i), Eqs. (2) and (3) recover exactly the Schrödinger equation for the total density matrix of the system-bath composite ρ_T [37],

$$\rho_T = \langle\rho_S\rho_B\rangle \equiv \int_{t_0}^{t}\mathcal{D}\bar{\boldsymbol{\eta}}\mathcal{D}\boldsymbol{\eta}e^{-\int_{t_0}^{t}\bar{\eta}_\tau\eta_\tau d\tau}\rho_S\rho_B, \tag{4}$$

where $\langle\cdots\rangle$ denotes the stochastic average over all the AGFs, with $\bar{\boldsymbol{\eta}} \equiv \{\bar{\eta}_{j\tau}\}$ and $\boldsymbol{\eta} \equiv \{\eta_{j\tau}\}$. To obtain the physical observables, we need to acquire the reduced system density matrix $\rho = \mathrm{tr}_B(\rho_T) = \langle\tilde{\rho}_S\rangle$ with $\tilde{\rho}_S \equiv \rho_S\mathrm{tr}_B(\rho_B)$. An arbitrary system observable O is evaluated via $O = \mathrm{tr}_S(\hat{O}\rho)$. Here, tr_B (tr_S) denotes the trace over the bath (system) subspace.

Mapping (ii): Capturing non-Markovian bath memory.—The influence of non-Markovian bath memory on the reduced system dynamics is captured by $\mathrm{tr}_B(\rho_B)$. For a noninteracting bath, it can be explicitly evaluated by solving Eq. (3) using the Magnus expansion [48], and the result includes the following memory-convoluted AGFs [37]:

$$g_t^- = \int_{t_0}^{t}\{[C^+(t-\tau)]^*\eta_{4\tau} - iC^-(t-\tau)\eta_{2\tau}\}d\tau,$$
$$g_t^+ = \int_{t_0}^{t}\{[C^-(t-\tau)]^*\bar{\eta}_{3\tau} - iC^+(t-\tau)\bar{\eta}_{1\tau}\}d\tau, \tag{5}$$

where the bath correlation functions $C^\pm(t-\tau)$ are related to the bath spectral function via the fluctuation-dissipation theorem [37]. Inclusion of the influence of bath leads to the following rigorous SEOM for $\tilde{\rho}_S$:

$$\dot{\tilde{\rho}}_S = -i[H_S,\tilde{\rho}_S] + e^{-i\pi/4}\{\hat{c}^\dagger g_t^- - g_t^+\hat{c},\tilde{\rho}_S\} + e^{-i\pi/4}(\hat{c}^\dagger\eta_{1t} + \bar{\eta}_{2t}\hat{c})\tilde{\rho}_S + e^{i\pi/4}\tilde{\rho}_S(\hat{c}^\dagger\eta_{3t} + \bar{\eta}_{4t}\hat{c}). \tag{6}$$

Here, the memory-convoluted AGFs $\{g_t^\pm\}$ and the instantaneous AGFs $\{\eta_{jt},\bar{\eta}_{jt}\}$ characterize the mean force and random force exerted by the bath, respectively [49].

Being the result of the mapping (ii), Eq. (6) is formally exact. However, the practical use of Eq. (6) faces the fundamental difficulty of realizing the AGFs. Such difficulty has prohibited any direct numerical application of Eq. (6) or its analogues [43,47].

Mapping (iii): Representing AGFs by c numbers and pseudolevels.—Now we show it is possible to represent g numbers by operable quantities and obtain accurate results. Consider a prototypical SEOM:

$$\dot{y} = y\left(D(t)\eta_t + \int_{t_0}^{t}C(\tau)\bar{\eta}_\tau d\tau\right), \tag{7}$$

where $C(t)$ and $D(t)$ are known functions. We propose by intuition a mapping as follows:

$$\eta_t \mapsto v_tX^-, \qquad \bar{\eta}_t \mapsto v_tX^+. \tag{8}$$

Here, the c-number noises $\{v_t\}$ account for the stochastic amplitudes of the AGFs, while the pseudo-operators $X^\pm$ trace the time order of the AGFs. Specifically, $X^\pm$ are defined in the space $S = \{-1,0,1\}$. Let $\tilde{y} = \sum_{l\in S}\tilde{y}^{[l]}$. The action of $X^\pm$ on $\tilde{y}^{[l]}$ gives $\tilde{y}^{[l]}X^\pm = \delta_l^\pm\tilde{y}^{[l\pm1]}$, with $\delta_0^\pm = \delta_{-1}^+ = -\delta_1^- = 1$ and $\delta_{-1}^- = \delta_1^+ = 0$. The mapping of Eq. (8) converts Eq. (7) to a conventional stochastic differential equation:

$$\dot{\tilde{y}} = \tilde{y}\left(D(t)v_tX^- + \int_{t_0}^{t}C(\tau)v_\tau d\tau X^+\right). \tag{9}$$

Interestingly, the average of $\tilde{y}$, defined by $\langle\tilde{y}\rangle \equiv \mathcal{M}(\tilde{y}^{[0]})$ with $\mathcal{M}$ denoting the stochastic average over $\{v_t\}$, reproduces exactly $\langle y\rangle$, the average of y over $\{\bar{\eta}_\tau,\eta_\tau\}$ [37].

In general, the mapping of Eq. (8) is not guaranteed to be exact, because the space S is drastically smaller than that of the AGFs. For Eqs. (5) and (6), which involve the convolution of memory, the finiteness of S may cause a loss of memory when tracing the cumulative influence of the AGFs. This is to be analyzed below.

We now apply the mapping of Eq. (8) to the AGFs in Eq. (6), i.e., $\eta_{jt} \mapsto v_{jt}X_j^-$ and $\bar{\eta}_{jt} \mapsto v_{jt}X_j^+$, where $\{v_{jt}\}$ are Gaussian white noises, while $X_j^\pm$ are pseudo-operators defined in the space $S_j = \{-1,0,1\}$. We further set $X_3^\pm = X_1^\pm$ and $X_4^\pm = X_2^\pm$. Like the g numbers, $X_j^\pm$ mutually anticommute. The non-Markovian bath memory is characterized

by the memory-convoluted c-number fields $\{\tilde{g}_t^{\pm}\}$, which are obtained via replacing $\eta_{j\tau}$ and $\bar{\eta}_{j\tau}$ in Eq. (5) by $v_{j\tau}$. Denote also

$$Y_1 \equiv v_{1t}X_1^- + \tilde{g}_t^- X_2^-, \qquad Y_2 \equiv v_{2t}X_2^+ - \tilde{g}_t^+ X_1^+,$$
$$Y_3 \equiv v_{3t}X_1^- - i\tilde{g}_t^- X_2^-, \qquad Y_4 \equiv v_{4t}X_2^+ + i\tilde{g}_t^+ X_1^+. \tag{10}$$

Define $\tilde{\rho}_S = \sum_{l_1\in S_1}\sum_{l_2\in S_2}\tilde{\rho}_S^{[l_1 l_2]}$ in the space $V \equiv V_S \otimes S_1 \otimes S_2$, where V_S is the system subspace. $X_j^{\pm}$ can act to the left or right of $\tilde{\rho}_S$, and the results of the actions are detailed in the Supplemental Material [37]. We thus map Eq. (6) to a numerically feasible SEOM:

$$\dot{\tilde{\rho}}_S = -i[H_S, \tilde{\rho}_S] + e^{-i\pi/4}(\hat{c}^\dagger Y_1 + Y_2\hat{c})\tilde{\rho}_S + e^{i\pi/4}\tilde{\rho}_S(\hat{c}^\dagger Y_3 + Y_4\hat{c}), \tag{11}$$

with the initial condition $\tilde{\rho}_S(t_0) = \tilde{\rho}_S^{[00]}(t_0)$. The statistical average of $\tilde{\rho}_S$ is obtained via $\rho = \langle\tilde{\rho}_S\rangle \equiv \mathcal{M}(\tilde{\rho}_S^{[00]})$.

Equation (11) is the result of the mapping (iii). The space S_j represents a pseudolevel, with its three elements (1, 0, and -1) labeling a single-particle, vacuum, and single-hole pseudo-Fock-states, respectively. The action of $X_j^+\hat{c}$ ($\hat{c}^\dagger X_j^-$) on $\tilde{\rho}_S$ can be interpreted as the transfer of a particle (hole) from the system to the jth pseudolevel. Thus, the space $S_1 \otimes S_2$ serves as a register to record the time order of the stochastic forces.

Important features of the fermionic SEOM.—If the system dynamics spans N_t time steps, it would take $8N_t$ mutually anticommuting matrices of the size $2^{8N_t} \times 2^{8N_t}$ to represent all the AGFs in Eq. (6). In contrast, after the mapping (iii), it only requires 4 matrices of the size $3^2 \times 3^2$ to represent all the pseudo-operators in Eq. (11). Clearly, the mapping (iii) drastically reduces the size of the auxiliary space, and thus makes the stochastic simulation of fermionic dissipative dynamics possible.

We now analyze how the reduced size of the auxiliary space affects the exactness of Eq. (11) by making connection to the fermionic HEOM formalism [18,50]. The basic variables of HEOM are auxiliary density operators (ADOs) constructed based on an exponential unraveling of the bath correlation functions. It can be proved that an arbitrary ADO can be retrieved exactly from the formal solution of Eq. (6) [37]; i.e., Eq. (6) is formally equivalent to the rigorous fermionic HEOM.

As the result of the mapping (iii), Eq. (11) is formally equivalent to a simplified version of HEOM (sim-HEOM) [37,50], in which all the interference ADOs are preset to zero, rather than to the full HEOM. In the context of Eq. (11), the definition of an interference ADO involves two or more identical pseudo-operators $X_j^{\pm}$. Since each pseudolevel accommodates at most one particle or hole, the repetitive actions of a same pseudo-operator $X_j^{\pm}$ on $\tilde{\rho}_S$ must yield zero [37]. It is thus clear that the mapping (iii) is intrinsically approximate, as it may cause loss of memory when a same particle-transfer event occurs more than 2 times in a row.

The SEOM of Eq. (11) and the sim-HEOM share the following common features [50]: (a) For general non-interacting systems, they yield the exact reduced *single-particle* density matrix and any system observable. Consequently, despite the approximation adopted in the mapping (iii), the resulting SEOM of Eq. (11) can still yield exact dissipative dynamics. (b) For general interacting systems, the resulting dissipative dynamics are in principle approximate, because the interference ADOs can be important for a quantitative description of the many-body correlation effects. Nevertheless, as will be shown below, Eq. (11) can still give accurate prediction on the dissipative dynamics of an interacting open system.

Extension of Eqs. (6) and (11) to general multilevel systems is straightforward, and the mappings (i)–(iii) as well as the above analysis remain valid [37].

Numerical example: Stochastic simulation of dissipative electron dynamics.—We now demonstrate the practicality and accuracy of the fermionic SEOM by studying a single-impurity Anderson model. The impurity (system) and the reservoir (bath) are represented by $H_S = \sum_{s=\uparrow,\downarrow}\epsilon_s\hat{n}_s + U\hat{n}_\uparrow\hat{n}_\downarrow$ and $H_B = \sum_{ks}\epsilon_{ks}\hat{n}_{ks}$, respectively, where $\hat{n}_s$ and $\hat{n}_{ks}$ are electron number operators, and U is the

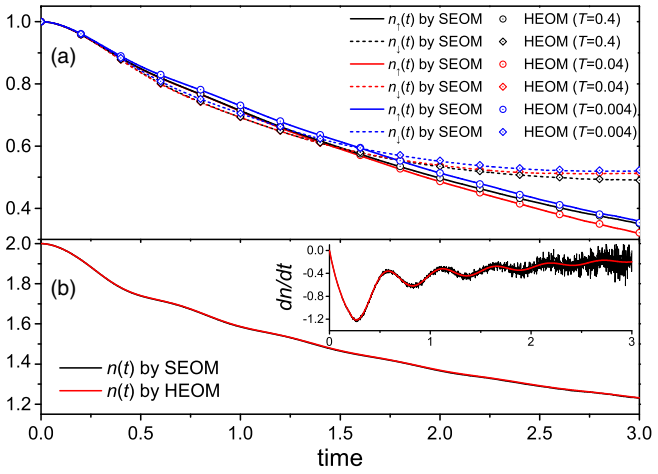

FIG. 3. (a) Time evolution of $n_s(t)$ calculated with the SEOM and HEOM methods. The parameters adopted are (in arbitrary unit): $\epsilon_\uparrow = 0.5$, $\epsilon_\downarrow = -0.5$, $U = 5$, $\Gamma = 0.5$, $\Omega = 0$, and $W = 5$. The Euler-Maruyama algorithm [52] is employed to solve the SEOM with a time step of $dt = 0.001$. The number of trajectories is $N_{\rm traj} = 5 \times 10^6$ for all lines. (b) $n(t) = n_\uparrow(t) + n_\downarrow(t)$ calculated with the SEOM and HEOM methods. The impurity level energy is shifted by $\Delta\epsilon = -5.0$ during the time interval $0.1 < t < 0.2$. Other parameters adopted are (in arbitrary unit): $\epsilon_\uparrow = \epsilon_\downarrow = -2.5$, $U = 10$, $\Gamma = 0.5$, $\Omega = 0$, $W = 5$, and $T = 0.01$. We choose $dt = 0.001$ and $N_{\rm traj} = 1 \times 10^6$ for SEOM calculations. To reveal the stochastic nature of the calculated $n(t)$, we display its time derivative (dn/dt) in the inset of (b), so that the stochastic variance becomes recognizable.

electron-electron interaction energy. The bath memory is characterized by the hybridization function $\Delta_s(\omega) \equiv \pi \sum_k |t_{ks}|^2 \delta(\omega - \epsilon_{ks}) = (\Gamma/2)[W^2/((\omega-\Omega)^2+W^2]$, where Γ, Ω, and W are the effective impurity-reservoir coupling strength, and the reservoir band center and width, respectively.

Initially the impurity is doubly occupied by spin-up and -down electrons, and is isolated from the equilibrium reservoir. Then the turn-on of H_{SB} triggers the electron transfer between the impurity and the reservoir. The time evolution of $\rho(t)$ is obtained by solving a spin-resolved version of Eq. (11). The electron occupation number on the impurity is computed via $n_s(t) = \mathrm{tr}_S[\hat{n}_s \rho(t)]$, and compared against the highly accurate HEOM results in Fig. 3. Despite the appreciable value of U adopted, the results of our proposed SEOM agree remarkably with those of the full HEOM, with the relative deviations being less than 0.3% [37,51]. This is because the impurity-reservoir composite does not contain any strongly correlated state within the examined time window, and hence the simplified and the full HEOM give almost identical predictions [37].

Concluding remarks.—Regarding numerical efficiency, SEOM does not require the unraveling of $C^{\pm}(t)$, and hence its memory cost is drastically smaller than HEOM. This allows for exploring the ultralow-temperature regime which remains prohibitive for the present HEOM. Moreover, the trajectory-based algorithms could benefit from massive parallel computing techniques.

If the dissipative dynamics of an interacting system involves strongly correlated states, the mapping of Eq. (8) and the resulting SEOM may yield less accurate predictions. Even so, the proposed mapping strategy still lays a valuable foundation for future development of advanced SEOM methods. For instance, the electron-electron interaction in H_S may be further represented by stochastic c-number fields [53,54]. This will map the interacting system to an effectively noninteracting system and result in a formally exact SEOM. Alternatively, the many-body correlation manifested by the interference ADOs may be retrieved by a more sophisticated construction of the auxiliary spaces S_j.

Support from the Ministry of Science and Technology of China (Grants No. 2016YFA0400900 and No. 2016YFA0200600), the National Natural Science Foundation of China (Grants No. 21573202, No. 21633006, and No. 21373064), the MOE of China (111 Project Grant No. B18051), the Fundamental Research Funds for the Central Universities (Grant No. 2340000074), and the SuperComputing Center of USTC is gratefully acknowledged.

*xz58@ustc.edu.cn

[1] A. Einstein, Ann. Phys. (Berlin) **322**, 549 (1905).
[2] A. O. Caldeira and A. J. Leggett, Physica (Amsterdam) **121A**, 587 (1983).
[3] P. S. Riseborough, P. Hänggi, and U. Weiss, Phys. Rev. A **31**, 471 (1985).
[4] H. Grabert, P. Schramm, and G.-L. Ingold, Phys. Rep. **168**, 115 (1988).
[5] A. E. Kobryn, T. Hayashi, and T. Arimitsu, J. Phys. Soc. Jpn. **72**, 58 (2003).
[6] P. Hänggi and F. Marchesoni, Chaos **15**, 026101 (2005).
[7] H.-P. Breuer, E.-M. Laine, J. Piilo, and B. Vacchini, Rev. Mod. Phys. **88**, 021002 (2016).
[8] D. Tamascelli, A. Smirne, S. F. Huelga, and M. B. Plenio, Phys. Rev. Lett. **120**, 030402 (2018).
[9] Z. H. Li, N. H. Tong, X. Zheng, D. Hou, J. H. Wei, J. Hu, and Y. J. Yan, Phys. Rev. Lett. **109**, 266403 (2012).
[10] Á. Rivas, S. F. Huelga, and M. B. Plenio, Rep. Prog. Phys. **77**, 094001 (2014).
[11] I. de Vega and D. Alonso, Rev. Mod. Phys. **89**, 015001 (2017).
[12] B. M. Garraway, Phys. Rev. A **55**, 2290 (1997).
[13] B. M. Garraway, Phys. Rev. A **55**, 4636 (1997).
[14] Y. J. Yan, J. Chem. Phys. **140**, 054105 (2014).
[15] Y. Tanimura and R. Kubo, J. Phys. Soc. Jpn. **58**, 101 (1989).
[16] Y. Tanimura, Phys. Rev. A **41**, 6676 (1990).
[17] Y. A. Yan, F. Yang, Y. Liu, and J. S. Shao, Chem. Phys. Lett. **395**, 216 (2004).
[18] J. S. Jin, X. Zheng, and Y. J. Yan, J. Chem. Phys. **128**, 234703 (2008).
[19] H. Kleinert and S. V. Shabanov, Phys. Lett. A **200**, 224 (1995).
[20] L. Diósi and W. T. Strunz, Phys. Lett. A **235**, 569 (1997).
[21] J. T. Stockburger and H. Grabert, Phys. Rev. Lett. **88**, 170407 (2002).
[22] L. Diósi, J. Phys. A **21**, 2885 (1988).
[23] N. Gisin and I. C. Percival, J. Phys. A **25**, 5677 (1992).
[24] L. Diósi, N. Gisin, and W. T. Strunz, Phys. Rev. A **58**, 1699 (1998).
[25] I. Percival, *Quantum State Diffusion* (Cambridge University Press, Cambridge, England, 1999).
[26] W. T. Strunz, L. Diósi, and N. Gisin, Phys. Rev. Lett. **82**, 1801 (1999).
[27] J. Jing and T. Yu, Phys. Rev. Lett. **105**, 240403 (2010).
[28] D. Suess, A. Eisfeld, and W. T. Strunz, Phys. Rev. Lett. **113**, 150403 (2014).
[29] V. Link and W. T. Strunz, Phys. Rev. Lett. **119**, 180401 (2017).
[30] J. T. Stockburger and C. H. Mak, Phys. Rev. Lett. **80**, 2657 (1998).
[31] J. S. Shao, J. Chem. Phys. **120**, 5053 (2004).
[32] Y. Zhou, Y. A. Yan, and J. S. Shao, Europhys. Lett. **72**, 334 (2005).
[33] J. M. Moix and J. S. Cao, J. Chem. Phys. **139**, 134106 (2013).
[34] L. Zhu, H. Liu, and Q. Shi, New J. Phys. **15**, 095020 (2013).
[35] Y.-A. Yan and J. Shao, Phys. Rev. A **97**, 042126 (2018).
[36] J. Roden, A. Eisfeld, W. Wolff, and W. T. Strunz, Phys. Rev. Lett. **103**, 058301 (2009).

[37] See Supplemental Material at http://link.aps.org/supplemental/10.1103/PhysRevLett.123.050601 for detailed analytic analysis regarding the SEOM formulation and its relation to the HEOM theory.
[38] C. Barnett, R. F. Streater, and I. F. Wilde, J. Funct. Anal. **48**, 172 (1982).
[39] D. B. Applebaum and R. L. Hudson, Commun. Math. Phys. **96**, 473 (1984).
[40] A. Rogers, Commun. Math. Phys. **113**, 353 (1987).
[41] P. Hedegård and A. Caldeira, Phys. Scr. **35**, 609 (1987).
[42] X. Zhao, W. Shi, L.-A. Wu, and T. Yu, Phys. Rev. A **86**, 032116 (2012).
[43] M. Chen and J. Q. You, Phys. Rev. A **87**, 052108 (2013).
[44] W. Shi, X. Zhao, and T. Yu, Phys. Rev. A **87**, 052127 (2013).
[45] Y. Chen, J. Q. You, and T. Yu, Phys. Rev. A **90**, 052104 (2014).
[46] D. Suess, W. T. Strunz, and A. Eisfeld, J. Stat. Phys. **159**, 1408 (2015).
[47] C.-Y. Hsieh and J. S. Cao, J. Chem. Phys. **148**, 014103 (2018).
[48] D. J. Tannor, *Introduction to Quantum Mechanics: A Time-Dependent Perspective* (University Science Books, Sausalito, 2006).
[49] G. W. Ford, J. T. Lewis, and R. F. O'Connell, Phys. Rev. A **37**, 4419 (1988).
[50] L. Han, H. D. Zhang, X. Zheng, and Y. J. Yan, J. Chem. Phys. **148**, 234108 (2018).
[51] F. Mascherpa, A. Smirne, S. F. Huelga, and M. B. Plenio, Phys. Rev. Lett. **118**, 100401 (2017).
[52] P. E. Kloeden and E. Platen, *Numerical Solution of Stochastic Differential Equations* (Springer-Verlag Berlin Heidelberg, New York, 1992).
[53] J. Hubbard, Phys. Rev. Lett. **3**, 77 (1959).
[54] D. S. Golubev and A. D. Zaikin, Phys. Rev. B **59**, 9195 (1999).